Hemilabile and Redox-Active Quinone Ligands Unlock sp^3-Rich Couplings in Nickel-Catalyzed Olefin Carbosulfenylation

Zi-Qi Li,[a] Turki, M. Alturaifi, [b] Yilin Cao,[a] Matthew V. Joannou,[c] Peng Liu,*[b] and Keary M. Engle*[a]

[a] Dr. Z.-Q. Li; Y. Cao; Prof. K. M. Engle
Department of Chemistry
The Scripps Research Institute
10550 N. Torrey Pines Road, La Jolla, CA 92037, USA
E-mail: keary@scripps.edu

[a] T. M. Alturaifi; Prof. P. Liu; Prof
Department of Chemistry
University of Pittsburgh
219 Parkman Avenue, Pittsburgh, Pennsylvania 15260, USA
E-mail: pengliu@pitt.edu

[a] Dr. M. V. Joannou
Chemical Process Development
Bristol Myers Squibb
1 Squibb Drive, New Brunswick, NJ 08903, USA

Supporting information for this article is given via a link at the end of the document.

Abstract: A three-component coupling approach toward structurally complex dialkylsulfides is described via the nickel-catalyzed 1,2-carbosulfenylation of unactivated alkenes with organoboron nucleophiles and alkylsulfenamide (N–S) electrophiles. Efficient catalytic turnover is facilitated using a tailored N–S electrophile containing an *N*-methyl methanesulfonamide leaving group, allowing catalyst loadings as low as 1 mol%. Regioselectivity is controlled by a collection of monodentate, weakly coordinating native directing groups, including sulfonamides, amides, sulfinamides, phosphoramides, and carbamates. Key to the development of this transformation is the identification of quinones as a family of hemilabile and redox-active ligands that tune the steric and electronic properties of the metal throughout the catalytic cycle. Density functional theory (DFT) results show that the duroquinone (DQ) ligand adopts different coordination modes in different stages of the Ni-catalyzed 1,2-carbosulfenylation—binding as η^6 capping ligand to stabilize the precatalyst/resting state and prevent catalyst decomposition, binding as an X-type redox-active durosemiquinone radical anion to promote alkene migratory insertion with a less distorted square planar Ni(II) center, and binding as an L-type ligand to promote N–S oxidative addition at a relatively more electron-rich Ni(I) center.

Introduction

Organosulfur compounds possess unique properties that give rise to applications in medicinal chemistry,[1] material science,[2] and other scientific fields. Organosulfides, in which sulfur is in the +2 oxidation state, can be readily converted into sulfoxides, sulfones, and sulfoximines, which are likewise important functional groups in drug discovery[3] and other realms. Traditional methods for

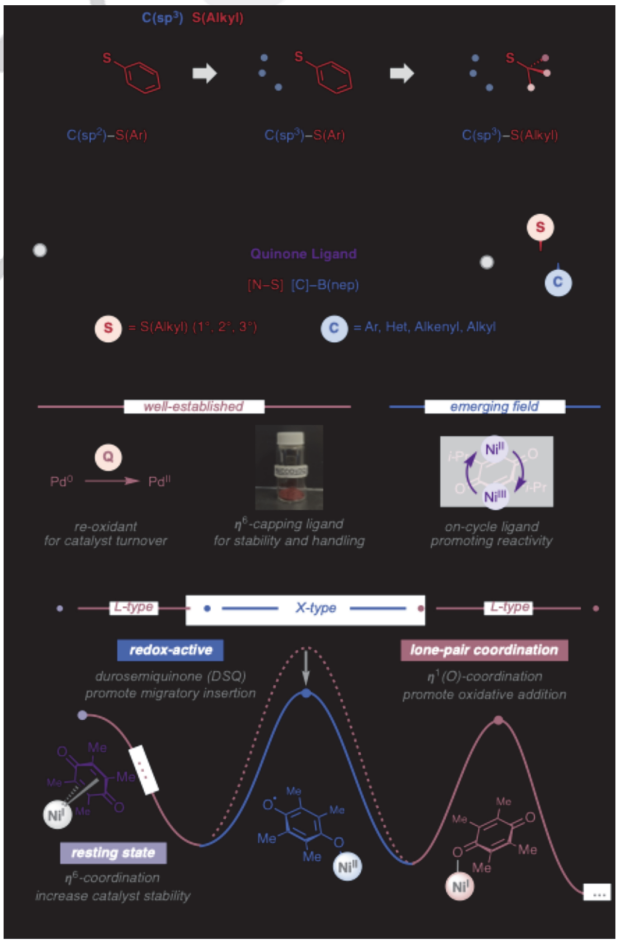

Scheme 1. Background and synopsis of current work.

transition-metal-catalyzed two-component C−S bond formation[4] can be categorized into two main redox paradigms. The Buchwald–Hartwig-type C–S coupling of organohalide electrophiles and organothiol nucleophiles represents a classical method for constructing C(sp^2)−S bonds.[5–6] Recently, umpolung C–S couplings have also emerged. These reactions utilize electrophilic sulfur reagents,[4h] which have favorable features, including their structural tunability, reduced tendency towards catalyst poisoning, and odorless nature. On this front, notable advancements have been achieved in transition-metal-catalyzed C−H functionalization reactions using electrophilic sulfonylthioate[7], sulfenamide[8], disulfide[9], and other sulfur surrogates[10].

While two-component umpolung C−S coupling has primarily focused on C(sp^2)−S(Aryl) bond formation[7–11], there is growing interest in gaining access to unexplored regions of C(sp^3)-rich organosulfur chemical space, specifically broadening the scope to include aliphatic carbon (C(sp^3)), and alkylsulfenyl (S(Alkyl)) reagents (Scheme 1A).[12] Whereas several recent studies have described catalytic C(sp^3)−S(Aryl) bond formation using radical-based approaches among others,[7b] methods that enable unsymmetrical dialkylsulfide synthesis through C(sp^3)−S(Alkyl) bond formation[13] remain rare. This scarcity is attributed to challenges associated with the stability of C(sp^3)−metal species as well as catalyst deactivation by the more electron-rich alkylthiolate species.

As part of our interest in olefin difunctionalization, [14–16] our group recently reported a nickel-catalyzed *syn*-selective 1,2-carbosulfenylation reaction of simple unactivated alkenes for the construction of vicinal C(sp^3)–C((Hetero)Aryl) and C(sp^3)–S(Ar) bonds enabled by tailored N–S electrophiles.[17] Extending the sulfur electrophile scope to encompass 1°, 2°, and 3° S(Alkyl) groups, and simultaneously augmenting the carbon nucleophile scope to alkenyl and alkyl groups would round out synthetic capabilities within this family of reactions (Scheme 1B). However, attempts to directly apply the N–S reagent tuning strategy from our prior work to *S(Alkyl) electrophiles* were unsuccessful. We surmised that the transition from S(Ar) and S(Alkyl) transfer present significant challenges due to demanding kinetic requirements on different elementary steps. This involves altering the electronic properties of the Ni intermediate in the N–S activation step, without interfering with other steps of the catalytic cycle. Recognizing that these challenges could not be addressed solely through reagent-based approach, we sought to identify an ancillary ligand to enable productive three-component S(Alkyl) coupling reactions.

Although it is well-established that a Ni(I)/Ni(III) oxidative addition is more feasible than corresponding Ni(II)/(IV) process[18], the preceding migratory insertion is more common with Ni(II) species than with Ni(I) speices.[15] Therefore, merging the two distinctive catalytic cycles through in-situ modulation of the metal's oxidation state may be critical for accomplishing transformations that are otherwise challenging. Taking inspiration from ubiquinone, nature's electron shuttle[19], the role of quinone and derivatives as electron reservoirs have been widely exploited in transition-metal catalysis. For decades, quinones have been employed as (co)oxidants[20–21] and/or promoters of reductive elimination in transition-metal catalysis (Scheme 1C, left panel).[22] Our laboratory has recently investigated quinones as electron-deficient diene ligands in the context of air-stable Ni(0) pre-catalysts (Scheme 1C, center panel).[23] With the commercialization of Ni(COD)(DQ) (COD = 1,5-cyclooctadiene; DQ = duroquinone), an increasing number of studies have noted improved reactivity compared to $Ni(COD)_2$.[24] These observations have led us to explore the catalytic potential of quinones beyond facilitating benchtop handling, focusing on their involvement in critical on-cycle elementary steps (Scheme 1C, right panel). Specifically, quinones can adopt different coordination modes that feature varying π-accepting character.[25] Additionally, the matching redox potentials between Ni(I)/Ni(II) and quinone/semiquinone could potentially enable seamless maneuvering among the metal's accessible oxidation states.[26] To the best of our knowledge, previous studies integrating two-way redox manipulation of nickel in the same catalytic cycle have mostly involved photocatalysis[27]. Ligand-controlled on-cycle oxidation state manipulation has not been reported. Herein, we report the discovery of quinones as *hemilabile*, *redox-active* ligands[28] that adopt different binding poses to promote distinct elementary steps in the nickel-catalyzed 1,2-carbosulfenylation reaction (Scheme 1D). An X-type η^1(O)-durosemiquinone (DSQ)-Ni(II) coordination formed through MLCT, is critical for the rate-limiting migratory insertion step. Meanwhile, electron-donating L-type η^1(O)-duroquinone coordination is important for the oxidative addition at a Ni(I) center. These findings complement a parallel study from our group in which quinones were shown to enable a series of 1,2-carboamidation reactions along a Ni(II)/Ni(III) redox coupling by serving as redox-inactive ligands that lower the activation barrier of migratory insertion through L-type η^1(O)-coordination.[29–30] Collectively, this emerging body of literature underscores the compelling potential of quinones as versatile ligands in catalysis, offering unique insights into their mechanistic roles in facilitating diverse transformations.

Results and Discussion

Reaction Discovery

To initiate the investigation, we selected alkenyl sulfonamide **1**, 4-fluorophenylboronic acid neopentyl glycol ester, and *n*-propylsulfenamide **S1** containing a 4-methoxy-*N*-methylbenzenesulfonamide leaving group as the three model reactants (Table 1).[17a] In preliminary experiments with $Ni(COD)_2$ as the precatalyst without added ligand, a maximum yield of 27% of the desired 1,2-carbosulfenylated **3aa** product was obtained, accompanied by 37% yield of the corresponding oxidative Heck byproduct **3aa'**. These results could not be improved despite extensive attempts to optimize the structure of the N–S reagent and reaction conditions. Thus, we turned attention toward ancillary ligands to improve product yield and suppress oxidative Heck byproduct formation. To our delight, quinones were identified as effective ligands for both purposes. Tetrasubstituted quinones were first evaluated, with DQ (**L1**) giving

Table 1. Optimization of reaction conditions.

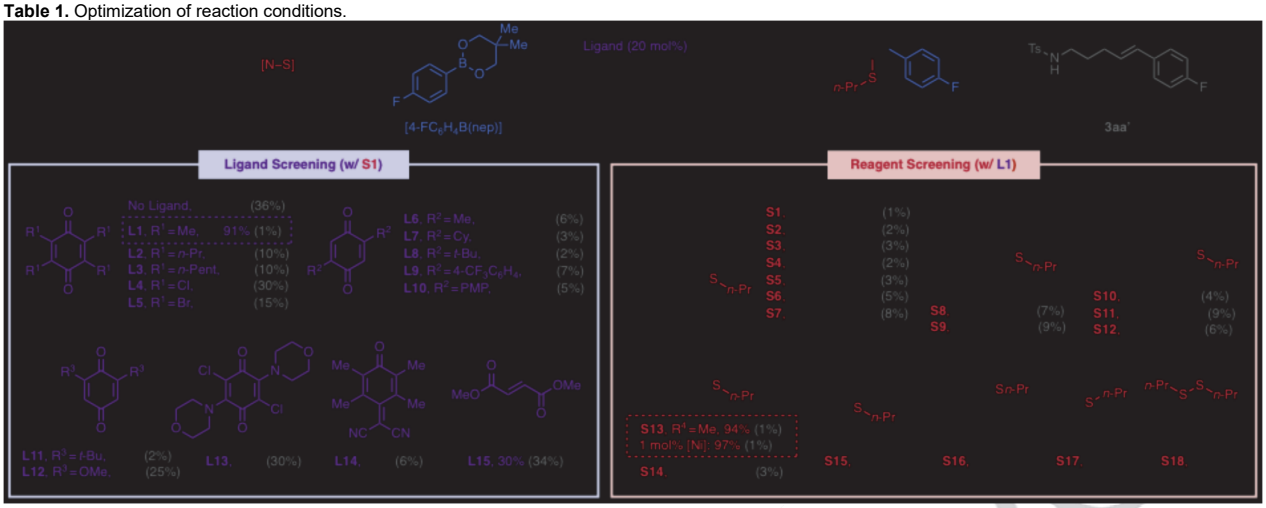

[a] Reactions performed on 0.1 mmol scale. $Ni(COD)_2$/**1**/Ligand/LiO*t*-Bu/[N–S]/4-F-C_6H_4B(nep) = 0.01/0.1/0.02/0.2/0.2/0.2 (mmol). THF (2.0 mL). Percentage yields represent ^1H NMR yields with benzyl 4-fluorobenzoate as internal standard. Yield in parenthesis represent ^1H NMR yields of byproduct **3aa'**. trace = less than 5%. [b] $Ni(COD)_2$/**1**/Ligand/LiO*t*-Bu/[N–S]/4-F-C_6H_4B(nep) = 0.001/0.1/0.005/0.2/0.15/0.2 (mmol). THF (1.0 mL). See supporting information for details.

the highest yield of 91% and minimizing oxidative Heck byproduct formation. Increasing the steric encumbrance (**L2**–**L3**) only gave moderate product yield and increased byproduct formation. More electron-deficient and more oxidizing quinones, such as chloranil and bromoanil (**L4**–**L5**), hampered the reaction, potentially due to electron transfer between catalyst and ligand.[26a,31] Subsequently, 2,5-disubstituted quinone ligands with alkyl (**L6**–**L8**) and aryl (**L9**–**L10**) groups were tested, giving moderate to good yield and less than 10% byproduct formation. Steric and electronic modifications to the substituents at these positions exhibited only a minor effect on reactivity. Excellent results were obtained with 2,6-di-*tert*-butylquinone (**L11**) as ligand, providing a potential alternative ligand to DQ. On the other hand, a more electron-rich 2,6-dimethoxy ligand (**L12**) resulted in significantly diminished yield and substantial oxidative Heck byproduct formation. Similar results were obtained with a 2,5-dichloro-3,6-dimorpholino ligand (**L13**). Dicyano *para*-quinone methide (**L14**) gave moderate yield when used as ligand. Other electron-deficient olefin ligands, such as dimethyl fumarate (DMFU, **L15**), furnished modest yield (30%) with more byproduct formation, underscoring the unique effectiveness of quinone ligands (see supporting information for detail). Pre-ligation of the DQ ligand to the nickel center led to slightly lower yield (see Supporting Information for details).

With DQ as the ligand, we next evaluated N–S reagents containing different leaving groups. Across sulfonamide leaving groups with different steric and electronic properties (**S1**–**S12**); yields of the 1,2-carbosulfenylated product consistently exceeded 70% with less than 10% byproduct formation. Minor detrimental effects were noted with electron-withdrawing groups on the aryl ring (**S5**–**S7**) and with sterically bulky substituents on either the arylsulfonyl or the *N*-alkyl moieties (**S8**–**S9**, **S11**). The best yield and selectivity were obtained using **S13**, which features an *N*-methyl methansulfonamide leaving group. At 10 mol% catalyst loading, 94% yield of **3aa** was recorded. Whereas other N–S reagents (e.g., **S1**) required catalyst loadings of 10 mol% for high yield, with N–S reagent **S13** and DQ as the ligand, the catalyst loading could be lowered to 1 mol% without a drop in yield (see supporting information for detail). Consistent with our prior findings[17a], N–S reagents with *N*-phenyl benzene sulfonamide as leaving group (**S15**) failed to yield the desired product due to a substantially weaker N–S bond, whereas reagent with phthalimide as leaving group (**S16**) exhibited low solubility. Sulfenylthioate (**S17**) and disulfide (**S18**) reagents also did not form the desired product and could be recovered at the end of the reaction.

Electrophile Scope

Having optimized a high-yielding and selective method, we turned attention to evaluating a series of primary, secondary, and tertiary alkylsulfenyl (–SAlkyl) electrophiles (Table 2). Primary alkylsulfenyl groups were first evaluated to understand reagent stability and functional group tolerance. It was found that various simple aliphatic –SAlkyl groups could be incorporated without issue (**3aa**–**3ad**). In general, alkylsulfenyl groups with embedded oxygen and nitrogen substituents could also be incorporated in moderate to high yields, though in these cases the N–S reagent synthesis and stability merits discussion. Due to the use of electrophilic chlorinating agents such as SO_2Cl_2 and *N*-chlorosuccinimide (NCS) in the preparation of N–S electrophiles (see supporting information for detail), nucleophilic functional groups prone to undergoing chlorination were not tolerated in standard synthetic procedure. For instance, attempts to prepare N–S electrophiles with free –OH, –NH, or electron-rich arenes were unfruitful. Moreover, the highly reactive N–S bond is susceptible to nucleophilic substitution. As a result, attenuating the nucleophilicity of any tethered nitrogen substituents through suitable protecting/blocking groups is required (**3aj**–**3al**) to avoid reagent decomposition. Less nucleophilic oxygen-based functional groups, however, were generally well tolerated (**3ae**–**3ai**, **3am**–**3an**). It is worth mentioning that carbonyl groups bearing acidic α-H atoms were incompatible potentially due to the

in-situ generation of nucleophilic enolate moieties under the strong

Table 2. Electrophile scope.[a]

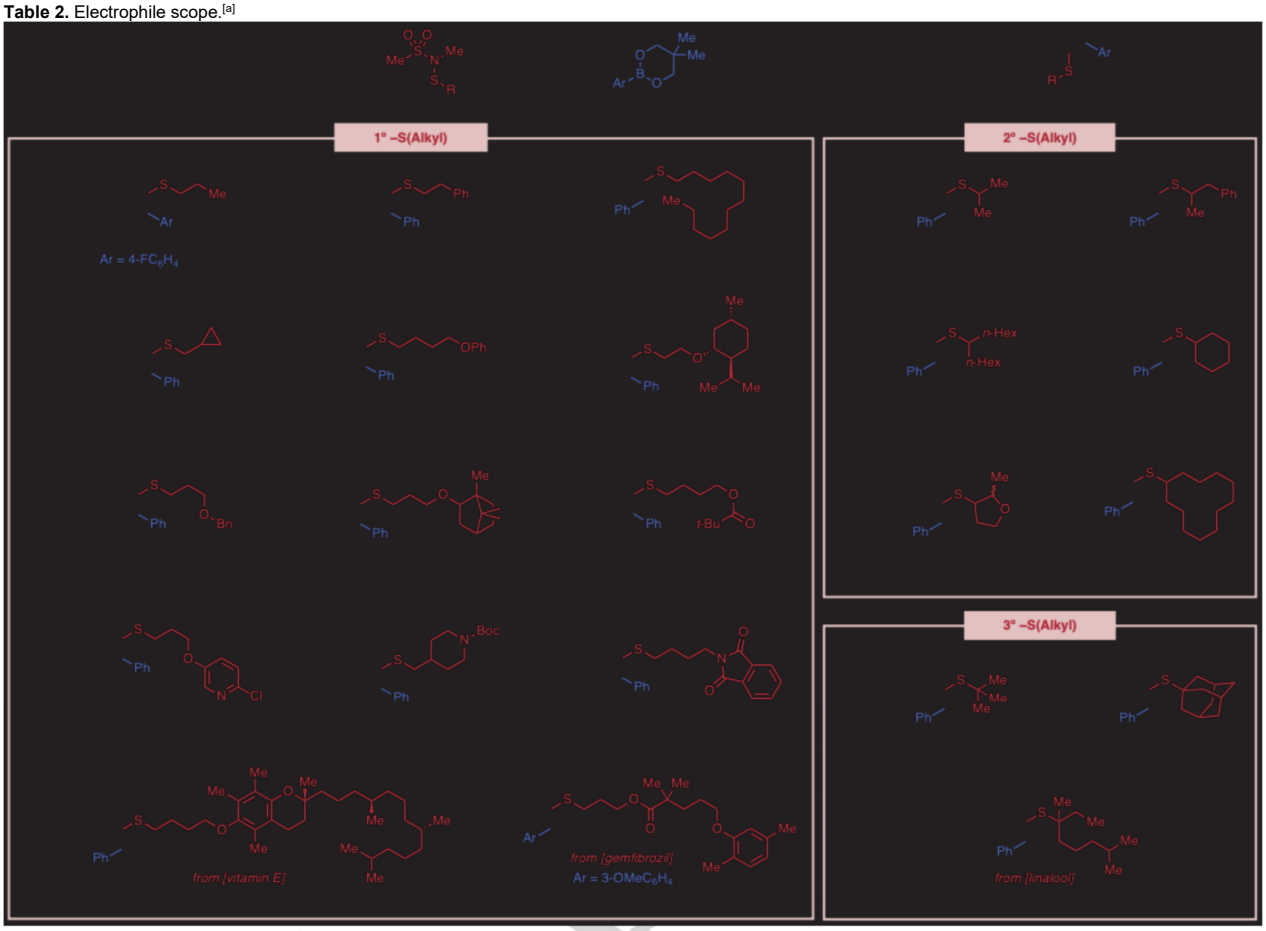

[a] Reactions performed on 0.1 mmol scale. Percentages represent isolated yields. [b] Reactions performed with N–S reagents bearing *N*-methylmethanesulfonamide as leaving groups at 1.0 mol% catalyst loading. [c] Reactions performed with N–S reagents bearing 4-methoxy-*N*-methylbenzenesulfonamide as leaving group at 2.0 mol% catalyst loading. In these cases an aromatic leaving group was selected to simplify purification of the product because *N*-methylmethanesulfonamide co-elutes with the product and is not UV-active. [d] Reactions performed with N–S reagents bearing *N*-methylmethanesulfonamide as leaving groups at 5.0 mol% catalyst loading. [e] Reactions performed with N–S reagents bearing *N*-methylmethanesulfonamide as leaving groups at 10.0 mol% catalyst loading. [f] Reactions performed with KOH (2.0 equiv) as base in place of LiO-*t*Bu (2.0 equiv).

alkaline conditions. Therefore, only pivaloyl groups and derivatives thereof (**3al**, **3an**) were able to provide the corresponding products. The number of methylene (–CH_2–) units between sulfur and the heteroatom moiety could be varied between two and four without evident influence on the reaction outcome, giving **3ae**–**3an** in good to excellent yields. Testing the compatibility of the chemistry with more structurally complex, biologically relevant structures, as exemplified in vitamin E (**3am**) and gemfibrozil (**3an**) derivatives furnished the desired product in good yields, despite a higher catalyst loading is required. Subsequently, N–S reagents with secondary –SAlkyl functional groups were tested. Both acyclic (**3ao**–**3aq**) and cyclic (**3ar**–**3at**) secondary alkylsulfenyl reagents proved compatible, with a minor adjustment of the base (from LiO*t*-Bu to KOH) proving necessary for selected acyclic alkylsulfenyl groups (**3ao**, **3aq**) and a cyclic alkylsulfenyl group with a large ring (**3at**). We hypothesize that this adjustment was required to accommodate the slightly higher conformational flexibility. Tertiary alkylsulfenyl groups also exhibited excellent reactivity, giving **3au**–**3aw** in good yields. To the best of our knowledge, transition-metal catalyzed installation of tertiary SAlkyl moiety with electrophilic sulfenylating reagents such as sulfonyl thiolates and disulfides remains scarcely reported due to challenging reagent activation.[7–11, 13]

Nucleophile Scope

Different organoboron nucleophiles were surveyed with **S13** as the standard sulfenylating reagent (Table 3). To showcase the catalytic efficacy of the optimized procedure, all reactions were performed at 1 mol% catalyst loading. We were pleased to find that high turnover numbers were consistently obtained. Arylboron coupling partners with electronically distinct substituents (from electron-donating –NHBoc to electron withdrawing –SO_2Me) on the *para*- position all gave the corresponding products in good to excellent yields (**3ba**–**3be**). Potentially reactive or inhibitory groups, for instance –NHBoc (**3ba**), –CHO (**3bb**), and –CN (**3bc**), were all compatible. Likewise, a *meta*-OMe substituent on the aryl nucleophile was incorporated in 92% yield (**3bf**). Furthermore,

substituents on the *ortho*- position were well tolerated with no evident deterioration in product yield accompanying the increase in steric encumbrance (**3bg**–**3bi**). Aryl boronic esters with fused heterocycles, specifically

Table 3. Nucleophile scope.[a]

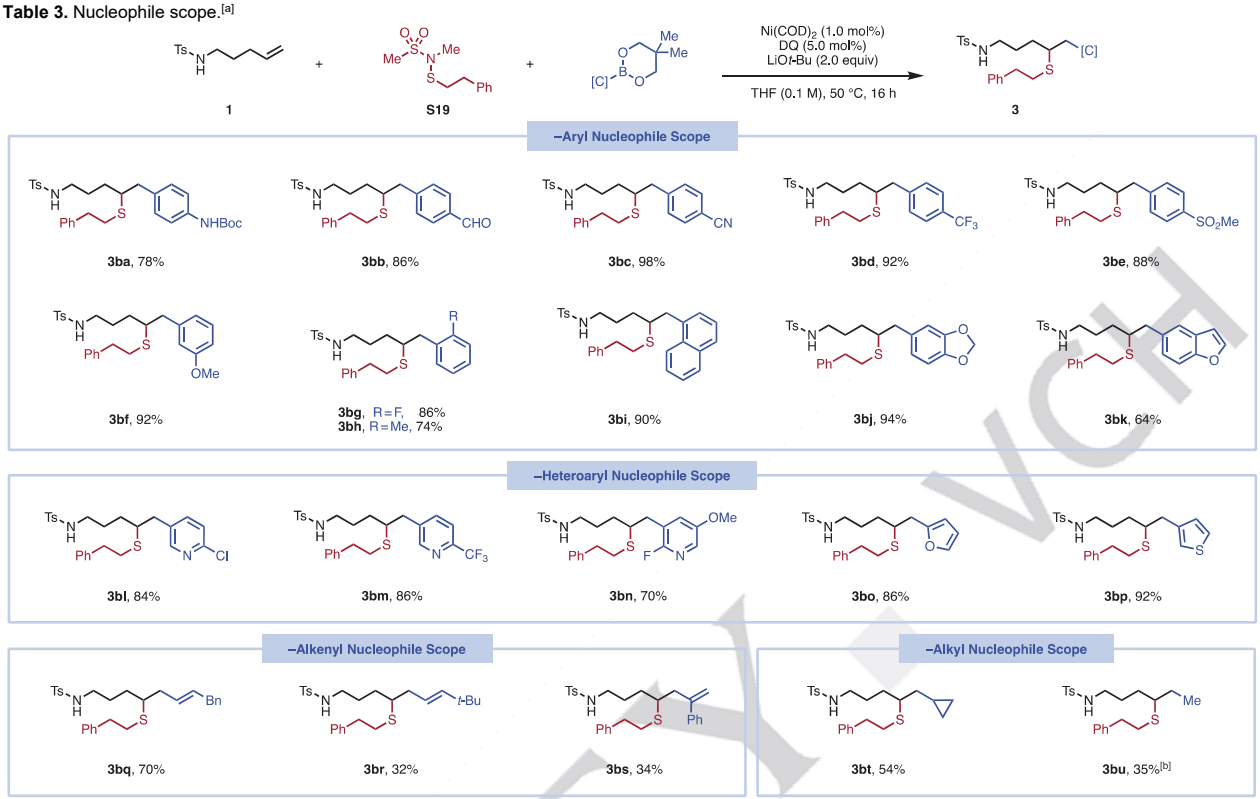

[a] Reactions performed on 0.1 mmol scale. Percentages represent isolated yields. [b] Reactions performed at 5.0 mol% catalyst loading. 5,5-diethyl-2-methyl-1,3,2-dioxaborinane was used as nucleophile.

benzodioxole and benzofuran moieties could be installed in 94% and 64% yield, respectively. We then explored of heteroaryl carbon nucleophiles. Electron-deficient pyridine-type nucleophiles could be introduced only in the presence of a substituent at 2-position to attenuate the coordinating strength of the N(sp^2) atom (**3bl**–**3bn**). Meanwhile, electron-rich heterocycles as exemplified by 2-furanyl and 3-thiofuranyl groups were also compatible (**3bo**–**3bp**), constituting an extension of the carbon nucleophile library as compared to our previous carbosulfenylation protocol where only aryl– and electron-deficient heterocycles were demonstrated.[17a] To our delight, the generality of the method held when alkenyl nucleophiles (**3bq**−**3bs**) and select alkyl nucleophiles (**3bt**−**3bu**) were examined, with the latter being rare examples of boron-based C(sp^3) nucleophiles in carbosulfenylation. Transitioning from −aryl, −heteroaryl, and −alkenyl coupling partners to −alkyl variants leads to products with higher C(sp^3) content, demonstrating the transformation's ability to form structurally complex organosulfides in a concise manner.

Alkene Scope

A series of alkenyl sulfonamides with different substitution patterns were evaluated (Table 4). When terminal alkenes were used, the reactivity could be maintained at low catalyst loading (**4a**–**4e**). Both benzenesulfonyl (**4a**–**4b**) and methanesulfonyl (**4c**) directing groups can furnish the corresponding products in prominent yields. While a branching on the β-position to the sulfonamide directing group resulted in moderate diastereoselectivity (**4d**), α-branching leads to significantly higher diastereoselectivity (**4e**). With internal alkenes as substrate, moderate to good yields and diastereoselectivities were obtained with a slightly higher catalyst loading (**4f**−**4k**). To illustrate the synthetic applicability of the described methodology, a removable sulfonamide directing group with 4-cyano substituent (Cs) was tested based on the well-established derivatization protocol involving a deprotection/amination process. Excellent yield whilst moderate diastereoselectivity was obtained (**4h**–**4i**). A skipped diene at the γ,δ- and ζ,η-positions was used to examine the chemoselectivity of the reaction, giving exclusively γ,δ-carbosulfenylated product **4k**. An endocyclic alkenyl sulfonamide gave **4l** in 27% yield with >20:1 diastereoselectivity (see supporting information for detail). A double carbosulfenylation reaction of a symmetric diene was achieved by adding excess coupling partners (4.0 equiv), furnishing **4m** in 80% yield. We also explored the potential of expanding the compatible directing functionalities. Alkenyl amides with a variety of functional groups were tolerated, giving **4n**–**4p** in moderate yields. The previously incompatible substrates, such as phosphinic amide (**4q**) and sulfinamide (**4r**) were adequately reactive directing groups. Particularly, with Ellman's chiral sulfinamide as directing group, a 7:1 diastereoselectivity was obtained in **4r**. Masked amine as in *tert*-butyl carbamate (**4s**) furnished the corresponding product in 42% yield. After extensive screening, we determined that a protic

hydrogen atom was required for the reaction to proceed. Notably, when primary alcohol was used as weakly protic directing group, 1,4-dioxane is required to obtain modest yield (**4t**). Non-directed

Table 4. Alkene scope.[a]

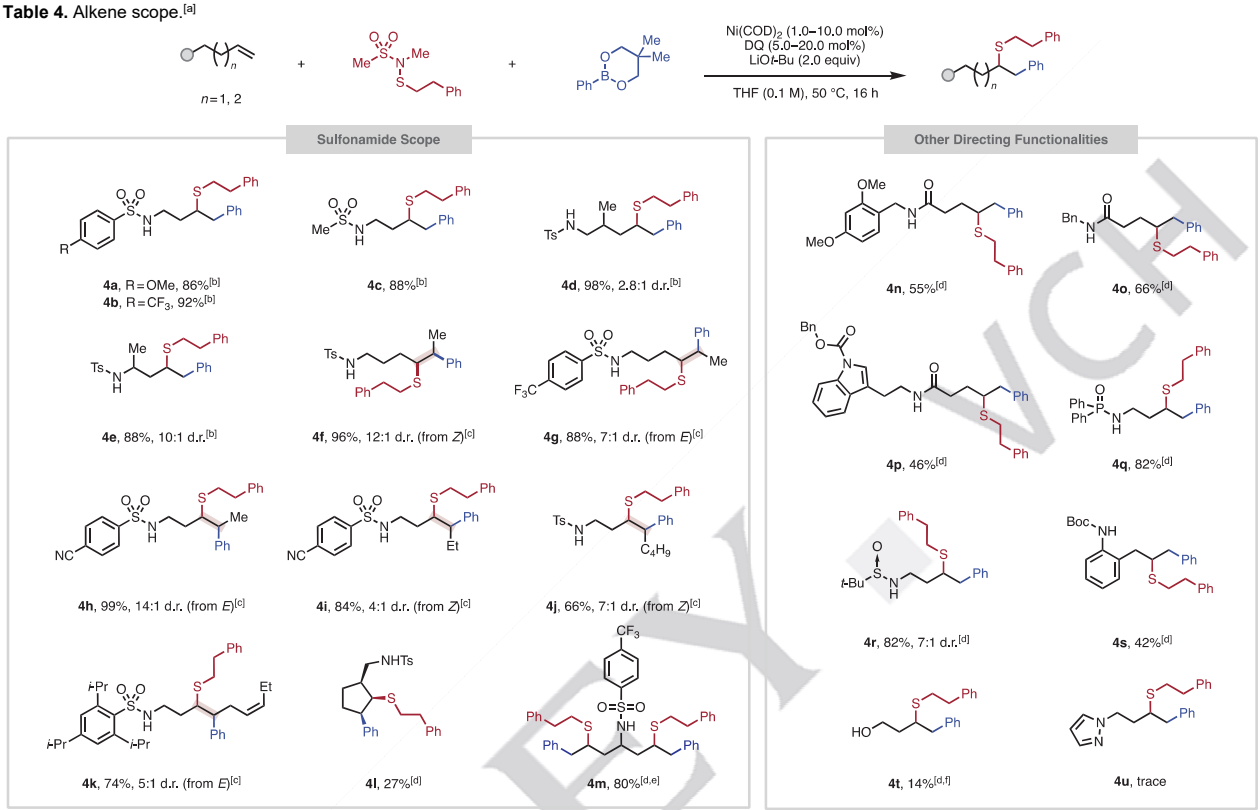

[a] Reactions performed on 0.1 mmol scale. Percentages represent isolated yields. [b] Reactions performed under 1 mol% catalyst loading. [c] Reactions performed under 5 mol% catalyst loading. [d] Reactions performed under 10 mol% catalyst loading. [e] Reaction performed with **S19** (4.0 equiv) and PhB(nep) (4.0 equiv). [f]Dioxane was used as solvent in place of THF.

alkenes, for instance, 1-phenylbutene and 1-dodecene were not operating, neither did azaheterocycles, which were deemed compatible in our prior studies.[15f, 17a] We reasoned that this distinction in substrate compatibility could be explained by the change in kinetic profile (see below).

Mechanistic Studies

The critical effect of quinone ligands in allowing integration of S(Alkyl) N–S electrophiles prompted us to investigate the origins of the enhanced reactivity using a combination of kinetics, density functional theory, and organometallic synthesis. First, we sought to understand the importance of in-situ ligation versus pre-ligation. To this end, we performed a series of initial rate experiments. While $Ni(COD)_2$ was only able to furnish 25% yield before catalyst deactivation, both pre-ligated Ni(COD)(DQ) and in-situ ligation of $Ni(COD)_2$ and duroquinone (DQ) gave excellent yield after extended reaction time (see Supporting Information for detail). However, an approximately twofold initial rate was observed with in-situ ligation, as in our standard conditions (Figure 1A). We rationalize these results on the basis that the Ni(I)/Ni(III) catalytic cycle requires an initial single-electron oxidation step that is more challenging from pre-ligated Ni(COD)(DQ) compared to $Ni(COD)_2$ (for proposed mechanism, see Supporting Information).

To further understand the role of quinone ligand in this reaction, both experimental and computational studies were performed particularly to explore the diverse coordination modes between the nickel catalyst and the quinone ligand. To this end, we treated Ni(COD)(DQ) with various bidentate ligands in an effort to study trends in coordination modes as a function of ligand properties. Whereas several weak-field ligands (e.g., 2,2'-bipyridine, 4,4'-*tert*-butyl-2,2'-bipyridine) led to formation of insoluble complexes that could not be characterized, clear ligand exchange was observed when a series of stronger-field bisphosphine ligands were used, revealing a distribution between η^6 and η^2 coordination modes in solution as a function of the ligand bite angle (see Supporting Information for detail). With 1,2-bis(diphenylphosphino)ethane (dppe), we were able to characterize both coordination modes in the solid state through X-ray crystallography.[32] Though it should be emphasized that these ligands and conditions are not directly relevant to the catalytic conditions, the results nevertheless demonstrate multiple co-existing coordination modes under ambient conditions. Taking inspiration from the complexation study, we were prompted to profile the complete illustration of Ni-

quinone coordination behavior along the reaction pathway. Because Ni complexes in the proposed catalytic cycle[17a] have different oxidation states, numbers of *d* electrons, and distinct steric properties, we surmised that the DQ ligand may adopt different coordination modes to facilitate different elementary steps.[33] We carefully considered several possible DQ coordination modes (Figure 1B) for each intermediate and transition state in the reaction of alkenyl sulfonamide **1**, phenylboronic acid neopentyl glycol ester, and the N–S electrophile **S20** by means of density functional theory (DFT).[34] The most favorable intermediates and transition states involved in each elementary step are shown in the reaction free energy profile in Figure 1C. The electron-rich π-

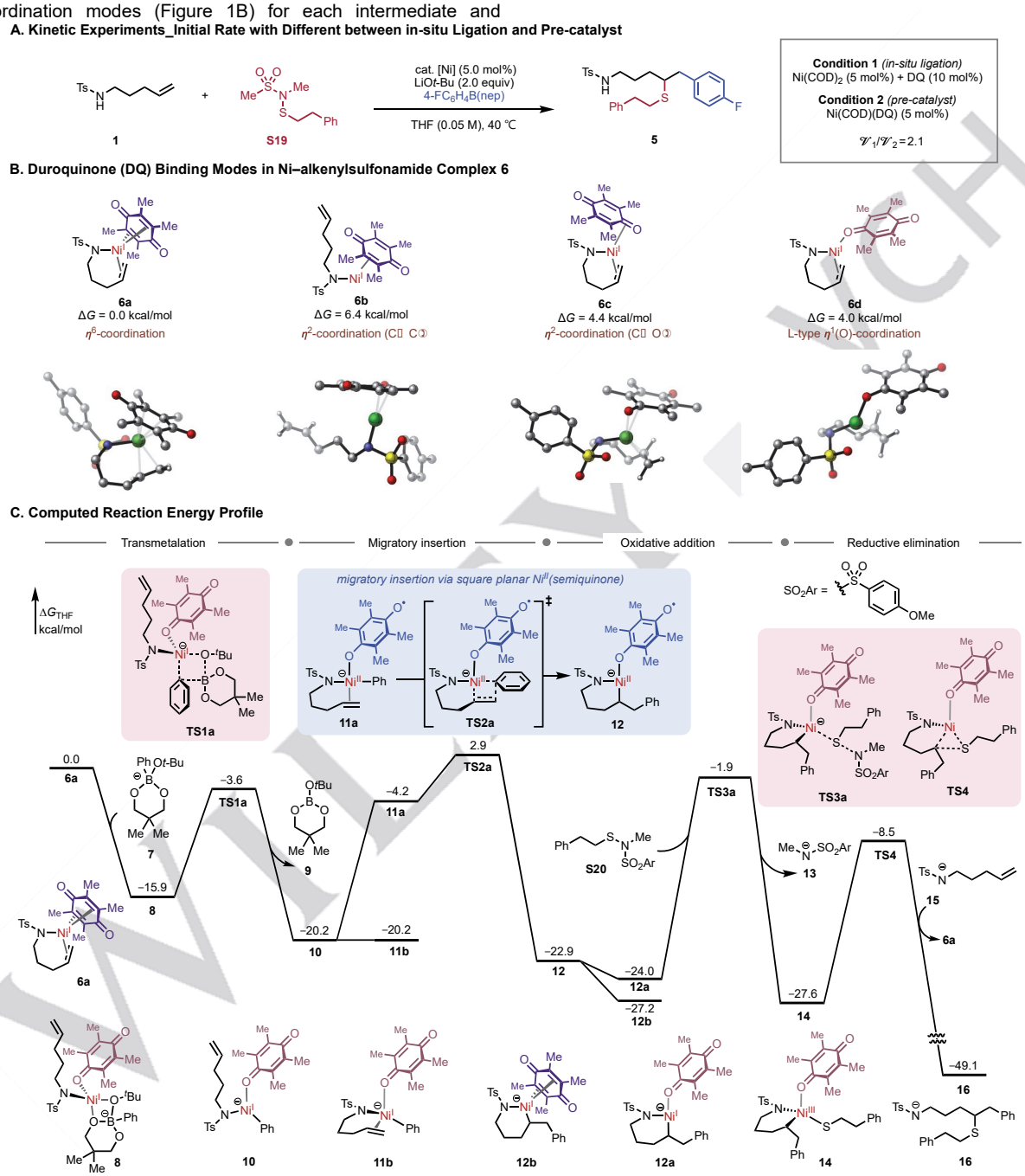

Figure 1. A) Initial rate experiments. B) Potential coordination modes of the hemilabile DQ ligand. C) Computed reaction energy profile of the Ni catalyzed 1,2-carbosulfenylation of alkene **1** with duroquinone ligand (**L1**). All Gibbs free energies are with respect to the Ni–alkenyl sulfonamide complex **6a** and phenyl boronate anion **7**.

alkene sulfonamide–Ni(I)complex **6** prefers an η^6 DQ coordination mode, in which the Ni center is simultaneously coordinated to the six carbons of the quinone ring (Figure 1B). According to our computational studies, this η^6 coordination mode is

thermodynamically more stable by at least 2.3 kcal/mol than other possible coordination modes such as the η^2(C=C) bound **6b**, the η^2(C=O) bound **6c**, and the η^1(O)-bound **6d**. Upon binding of **6a** with phenylboronate **7**, a tetrahedral complex **8** is formed where the DQ binds via an L-type η^1-coordination with the carbonyl oxygen (Figure 1C). The coordination of alkenyl sulfonamide **1** leads to a faster transmetalation of the phenyl group to the nickel center, as the transmetalation from a Ni(I) complex without sulfonamide coordination results in a higher activation barrier by 25.5 kcal/mol (Figure S1). After transmetalation via **TS1a**, a phenyl Ni(I) complex **10** is formed, which also involves an η^1(O) DQ coordination. After coordination of the alkenyl group of the sulfonamide substrate to the Ni(I) center, a tetrahedral complex **11b** is formed, which also favors η^1 coordination of the DQ

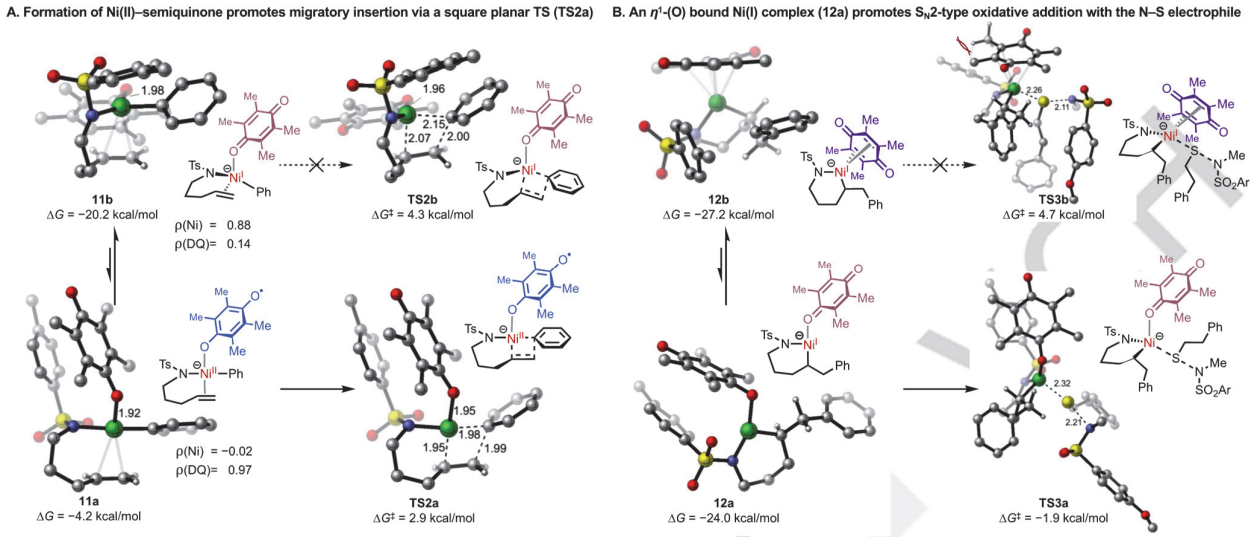

Figure 2. Preferred DQ coordination modes in (A) migratory insertion and (B) S_N2-type oxidative addition steps. Gibbs free energies are with respect to the Ni–alkenylsulfonamide complex **6a** and phenyl boronate anion **7.** Natural spin densities (ρ) were computed at the (U)ωB97X-D/6-311+G(d,p)–SDD(Ni)/SMD(THF) level of theory.

carbonyl oxygen to the electron-rich Ni. However, alkene migratory insertion cannot occur directly with **11b**, as it would require a highly distorted structure from the tetrahedral geometry. Instead, **11b** must isomerize to a square planar complex **11a** prior to migratory insertion. The computed natural spin densities from the Natural Bond Orbital (NBO) method[35] and the Ni–O(DQ) distance indicate that **11a** has a Ni(II) center bound to the oxygen atom of an X-type durosemiquinone radical anion (Figure 2A). The relatively short Ni–O distance in **11a** (1.92 Å) is consistent with those in other Ni^{II}–semiquinone complexes.[36] Additionally, the computed spin densities in complex **11a** indicate that the unpaired electron is primarily located on the DQ ligand (0.97), consistent with the open-shell character of the durosemiquinone radical anion ligand. In contrast, the spin densities in complex **11b** localize the unpaired electron on the Ni atom (0.88), with a comparatively minor contribution from the DQ ligand. This is in line with the characteristics associated with an L-type ligand bound to a Ni(I) center. The square planar Ni^{II}(DSQ) complex **11a** undergoes facile migratory insertion via a square planar transition state **TS2a**, which is only 7.1 kcal/mol higher in energy than **11a** and 23.1 kcal/mol higher than the three-coordinated π-alkene Ni(I) intermediate **10**. By contrast, the direct migratory insertion from tetrahedral Ni(I) complex **11b** via **TS2b** requires a higher barrier (TS isomers with other DQ coordination modes are even less favorable. See Figure S3). **TS2a** directly leads to a T-shaped Ni^{II}(DSQ) complex **12**, which then isomerizes to form a more stable Ni(I) complex **12b** featuring an η^6-coordination to DQ, as in other electron-rich and relatively less hindered Ni(I) intermediates in the catalytic cycle (*e.g.*, **6a**). Before the subsequent oxidative addition step with the N–S reagent **S20**, the DQ binding mode changes again to an L-type η^1(O) coordination, leading to a more electron-rich and less sterically hindered Ni(I) center in **12a**. These electronic and steric properties in the η^1(O)-bound **12a** facilitate subsequent S_N2-type oxidative addition via **TS3a**, where the Ni center maintains a tetrahedral geometry with the L-type DQ ligand. On the other hand, the activation barrier of the oxidative addition from the sterically congested η^6-coordinated **12b** via **TS3b** is 9.8 kcal/mol higher in energy than the activation barrier of **TS3a** via η^1(O)-bound **12a** (Figure 2B). Alternative oxidative addition pathways, including the η^2(C=C) coordination of DQ to Ni, are less stable than the oxidative addition via the η^1(O)-DQ coordination in **TS3a**. It is worth mentioning that the X-type directing group remains coordinated in the oxidative addition step, with the un-coordinated transition state being 40 kcal/mol higher in energy (Figure S4). The drastically higher energy barrier is in alignment with the requirement of X-type directing groups experimentally. Finally, the C(sp^3)–S(alkyl) reductive elimination transition state **TS4** occurs via an η^1(O)-coordinated Ni(III) intermediate **14** to yield the 1,2-carbosulfenylation product.

Taken together, the DFT calculations indicate that DQ serves as a redox-active and hemilabile ligand to promote multiple elementary steps in the carbosulfenylation catalytic cycle, which has not been previously documented in Ni(*para*-quinone) complexes to our knowledge.[23, 32–37]. Although the DQ ligand often adopts an η^6 coordination mode in several intermediates involved in the catalytic cycle, it changes to an L-type η^1(O) coordination to accommodate the sterically encumbered transmetalation transition state (**TS1a**) and electronically promote the S_N2-type

oxidative addition transition state with the N–S electrophile (**TS3a**). To mitigate the strain in the migratory insertion, an X-type semiquinone-bound Ni(II) complex is involved in a square planar migratory insertion transition state. Without these beneficial roles of DQ, multiple elementary steps can be more challenging. For example, the computed activation free energy of the migration insertion in the absence of the DQ ligand is 31.1 kcal/mol (see Figure S3), which is substantially higher than the activation free energy in the presence of DQ ($\Delta G^{\ddagger}$ = 23.1 kcal/mol, **TS2a**).

Conclusion

In conclusion, a family of quinone ligands were identified to enable nickel-catalyzed 1,2-carbosulfenylation of unactivated alkenes using tailored [N−S] reagents as electrophiles. The synthetic versatility of the method stems from the broad scope of 1°, 2°, and 3° S(Alkyl) electrophiles and (hetero)aryl, alkenyl, and alkyl nucleophiles. A large array of unactivated alkenes with native functionalities could be functionalized in a highly regioselective manner. The mechanistic merit of the reaction originates from the identification of the unique quinone/nickel coordination modes. DFT calculations reveal that the DQ ligand acts as a redox-active and hemilabile agent to facilitate multiple elementary steps in the carbosulfenylation catalytic cycle by adopting different coordination modes. The ligand's ability to change coordination modes promotes sterically encumbered transmetalation and electronically accelerates S_N2-type oxidative addition transition states, contributing to the efficiency of the overall catalytic process.

Conflict of Interest

The authors declare no conflict of interest.

Data Availability Statement

The data that support the findings of this study are available in the supplementary material of this article.

Acknowledgements

This work was financially supported by the National Science Foundation (CHE-2102550), the Alfred P. Sloan Fellowship program, and the Camille Dreyfus Teacher-Scholar program. We thank Bristol Myers Squibb for a Graduate Fellowship (Z.-Q.L.). Dr. Jason Chen is acknowledged for HRMS analysis. Computational calculations were carried out at the University of Pittsburgh Center for Research Computing and the Advanced Cyberinfrastructure Coordination Ecosystem: Services & Support (ACCESS) program, supported by NSF award numbers OAC-2117681, OAC-1928147 and OAC-1928224. We thank Dr. Roger Sommer (Bristol Myers Squibb) for assistance with X-ray crystallography.

Keywords: Carbosulfenylation • Ligand Design • Nickel • Redox-Active Ligands • Quinones

References

[1] a) E. A. Ilardi, E. Vitaku, J. T. Njardarson, *J. Med. Chem.* **2014**, *57*, 2832–2842. b) C. Zhao, K. P. Rakesh, L. Ravidar, W.-Y. Fang, H.-L. Qin, *Eur. J. Med. Chem.* **2019**, *162*, 679–734. c) M. Feng, B. Tang, S.-H. Liang, X. Jiang, *Curr. Top. Med. Chem.* **2016**, *16*, 1200–1216.

[2] K. Takimiya, I. Osaka, T. Mori, M. Nakano, *Acc. Chem. Res.* **2014**, *47*, 1493–1502.

[3] S. G. Modha, V. P. Mehta, E. V. van der Eycken, *Chem. Soc. Rev.* **2013**, *42*, 5042–5055.

[4] a) I. P. Beletskaya, V. P. Ananikov, *Chem. Rev.* **2011**, *111*, 1596–1636. b) C.-F. Lee, Y.-C. Liu, S. S. Badsara, *Chem. Asian J.* **2014**, *9*, 706–722. c) C. Shen, P. Zhang, Q. Sun, S. Bai, T. S. A. Hor, X. Liu, *Chem. Soc. Rev.* **2015**, *44*, 291–314. d) J.-X. Li, S.-R. Yang, W.-Q. Wu, H.-F. Jiang, *Org. Chem. Front.* **2020**, *7*, 1395–1417. e) N. Sundaravelu, S. Sangeetha, G. Sekar, *Org. Biomol. Chem.* **2021**, *19*, 1459–1482. f) Z.-W. Chen, R.-K. Bai, P. Annamalai, S.-S. Badsara, C.-F. Lee, *New J. Chem.* **2021**, *46*, 15–38. g) U. S. Kanchana, E. J. Diana, T. V. Mathew, *Asian J. Org. Chem.* **2022**, *11*, e202200038. h) Y.-F. Wei, W.-C. Gao, H.-H. Chang, X. Jiang, *Org. Chem. Front.* **2022**, *9*, 6684–6707.

[5] J. F. Hartwig, *Acc. Chem. Res.* **1998**, *31*, 852–860. b) G. Mann, D. Baranano, J. F. Hartwig, A. L. Rheingold, I. A. Guzei, *J. Am. Chem. Soc.* **1998**, *120*, 9205–9219. c) D. Baranano, J. F. Hartwig, *J. Am. Chem. Soc.* **2002**, *117*, 2937–2938. d) J. Louie, J. F.Hartwig, *J. Am. Chem. Soc.* **2002**, *117*, 11598–11599.

[6] Y.-C. Wong, T. T. Jayanth, C.-H. Cheng, *Org. Lett.* **2006**, *8*, 5613–5616. b) Y. Zhang, K. C. Ngeow, J.-Y. Ying, *Org. Lett.* **2007**, *9*, 3495–3498. c) A. Correa, M. Carril, C. Bolm, *Angew. Chem. Int. Ed.* **2008**, *47*, 2880–2883. d) E. Sperotto, G. P. van Klink, J. G. de Vries, G. van Koten, *J. Org. Chem.* **2008**, *73*, 5625–5628. e) M. S. Kabir, M. Lorenz, M. L. Van Linn, O. A. Namjoshi, S. Ara, J. M. Cook, *J. Org. Chem.* **2010**, *75*, 3626–3643. f) G. T. Venkanna, H. D. Arman, Z. J. Tonzetich, *ACS Catal.* **2014**, *4*, 2941–2950. g) T. Delcaillau, B. Morandi, *Chem.-Eur. J.* **2021**, *27*, 11823–11826. h) F. Zhang, Y. Wang, Y. Wang, Y. Pan, *Org. Lett.* **2021**, *23*, 7524–7528. i) I. Lindenmaier, R. Richter, I. Fleischer, *Org. Chem. Front.* **2024**. 2485–2493.

[7] W.-Q. Cai, Z.-H. Gu, *Org. Lett.* **2019**, *21*, 3204–3209. b) R. Mao, S. Bera, A. C. Turla, X. Hu, *J. Am. Chem. Soc.* **2021**, *143*, 14667–14675.

[8] P. Saravanan, P. Anbarasan, *Org. Lett.* **2014**, *16*, 848–851. b) R. Li, Y. Zhou, K.-Y. Yoon, Z. Dong, G. Dong, *Nat. Commun.* **2019**, *10,* 3555.

[9] L. D. Tran, I. Popov, O. Daugulis, *J. Am. Chem. Soc.* **2012**, *134*, 18237–18240. b) M. Iwasaki, M. Iyanaga, Y. Tsuchiya, Y. Nishimura, W.-J. Li, Z.-P. Li, Y. Nishihara, *Chem.-Eur. J.* **2014**, *20*, 2459–2462. c) G.-B. Yan, A. J. Borah, L.-G. Wang, *Org. Biomol. Chem.* **2014**, *12*, 9557–9561. d) Y.-X. Yang, W. Hou, L.-H. Qin, J.-J. Du, H.-J. Feng, B. Zhou, Y.-C. Li, *Chem. Eur. J.* **2014**, *20*, 416–420. e) C. Lin, D.-Y. Li, B.-J. Wang, J.-Z. Yao, Y.-H. Zhang, *Org. Lett.* **2015**, *17*, 1328–1331. f) M.-L. Li, J. Wang, *Org. Lett.* **2018**, *20*, 6490–6493. g) X. Wang, R.-H. Qiu, C.-Y. Yan, V. P. Reddy, L.-Z. Zhu, X.-H. Xu, S.-F. Yin, *Org. Lett.* **2015**, *17*, 1970–1973. h) S.-Y. Yan, Y.-J. Liu, B. Liu, Y.-H. Liu, Z.-Z. Zhang, B.-F. Shi, *Chem. Commun*. **2015**, *51*, 7341−7344.

[10] F.-J. Chen, G. Liao, X. Li, J. Wu, B.-F. Shi, *Org. Lett.* **2014**, *16*, 5644–5647. b) J.-X. Li, C.-S. Li, S.-R. Yang, Y.-N. An, W.-Q. Wu, H.-F. Jiang, *J.*

Org. Chem. **2016**, *81*, 7771–7783. c) X. Ge, F.-L. Sun, X.-M. Liu, X.-Z. Chen, C. Qian, S.-D. Zhou, *New J. Chem.* **2017**, *41*, 13175–13180.

[11] C. Savarin, J. Srogl, L. S. Liebeskind, *Org. Lett.* **2002**, *4*, 4309–4312. b) S. Yoshida, Y. Sugimura, Y. Hazama, Y. Nishiyama, T. Yano, S. Shimizu, T. Hosoya, *Chem. Commun.* **2015**, *51*, 16613–16616. c) S. Grassl, C. Hamze, T. J. Koller, P. Knochel, *Chem. Eur. J.* **2019**, *25*, 3752–3755. d) J.-C. Kang, Z.-H. Li, C. Chen, L.-K. Dong, S.-Y. Zhang, *J. Org. Chem.* **2021**, *86*, 15326–15334. e) Y. Wang, F. Zhang, Y. Wang, Y. Pan, *Eur. J. Org. Chem.* **2022**, e202101462.

[12] F. Lovering, J. Bikker, C. Humblet, *J. Med. Chem.* **2009**, *52*, 6752–6756.

[13] Y. Fang, T. Rogge, L. Ackermann, S.-Y. Wang, S.-J. Ji, *Nat. Commun.* **2018**, *9*. b) J. Li, S.-Y. Wang, S.-J. Ji, *J. Org. Chem.* **2019**, *84*, 16147–16156. c) J. Semenya, Y. Yang, E. Picazo, *J. Am. Chem. Soc.* **2024**, *146*, 4903–4912.

[14] J. Derosa, O. Apolinar, T. Kang, V. T. Tran, K. M. Engle, *Chem. Sci.* **2020**, *11*, 4287–4296. b) J. Diccianni, Q. Lin, T. Diao, *Acc. Chem. Res.* **2020**, *53*, 906–919. c) X. Qi, T. Diao, *ACS Catal.* **2020**, *10*, 8542–8556. d) R. Giri, S. KC, *J. Org. Chem.* **2018**, *83*, 3013–3022. e) S. Zhu, X. Zhao, H. Li, L. Chu, *Chem. Soc. Rev.* **2021**, *50*, 10836–10856. f) L. M. Wickham, R. Giri, *Acc. Chem. Res.* **2021**, *54*, 3415–3437.

[15] J. Derosa, V. T. Tran, M. N. Boulous, J. S. Chen, K. M. Engle, *J. Am. Chem. Soc.* **2017**, *139*, 10657–10660. b) W. Li, J. K. Boon, Y. Zhao, *Chem. Sci.* **2018**, *9*, 600–607. c) J. Derosa, R. Kleinmans, V. T. Tran, M. K. Karunananda, S. R. Wisniewski, M. D. Eastgate, K. M. Engle, *J. Am. Chem. Soc.* **2018**, *140*, 17878–17883. d) P. Basnet, S. KC, R. K. Dhungana, B. Shrestha, T. J. Boyle, R. Giri, *J. Am. Chem. Soc.* **2018**, *140*, 15586–15590. e) O. Apolinar, T. Kang, T. M. Alturaifi, P. G. Bedekar, C. Z. Rubel, J. Derosa, B. B. Sanchez, Q. N. Wong, E. J. Sturgell, J. S. Chen, S. R. Wisniewski, P. Liu, K. M. Engle, *J. Am. Chem. Soc.* **2022**, *144*, 19337–19343. f) Y. Cao, Z.-Q. Li, K. M. Engle, *Tetrahedron Lett.* **2023**, *132*, 154764.

[16] K. M. Logan, S. R. Sardini, S. D. White, M. K. Brown, *J. Am. Chem. Soc.* **2018**, *140*, 159–162. b) J. Derosa, V. A. van der Puyl, V. T. Tran, M. Y. Liu, K. M. Engle, *Chem. Sci.* **2018**, *9*, 5278–5283. c) V. A. van der Puyl, J. Derosa, K. M. Engle, *ACS Catal.* **2019**, *9*, 224–229. d) T. Kang, N. Kim, P. T. Cheng, H. Zhang, K. Foo, K. M. Engle, *J. Am. Chem. Soc.***2021**, *143*, 13962–13970. e) R. K. Dhungana, V. Aryal, D. Niroula, R. R. Sapkota, M. G. Lakomy, R. Giri, *Angew. Chem. Int. Ed.* **2021**, *60*, 19092–19096. f) T. Kang, J. M. González, Z.-Q. Li, K. Foo, P. T. W. Cheng, K. M. Engle, *ACS Catal.***2022**, *12*, 3890–3896.

[17] Z.-Q. Li, Y. Cao, T. Kang, K. M. Engle, *J. Am. Chem. Soc.* **2022**, *144*, 7189–7197. b) Z.-Q. Li, W.-J. He, H.-Q. Ni, K. M. Engle, *Chem. Sci.* **2022**, *13*, 6567–6572.

[18] Y. Aihara, N. Chatani, *J. Am. Chem. Soc.* **2013**, *135*, 5308–5311. b) J. R. Bour, N. M. Camasso, M. S. Sanford, *J. Am. Chem. Soc.* **2015**, *137*, 8034–8037. c) Y. Li, L. Zou, R. Bai, Y. Lan, *Org. Chem. Front.* **2018**, *5*, 615–622.

[19] D. Casagrande, P. H. Waib, A. A. Jordão Júnior, *J. Nutr. Intermed. Metab.* **2018**, *13*, 26–32.

[20] A. Vasseur, J. Muzart, J. Le Bras, *Eur. J. Org. Chem.* **2015**, 4053–4069.

[21] For a book chapter see: B. V. Popp, S. S. Stahl, In *Organometallic Oxidation Catalysis*, *Vol. 22*, (Eds.: F. Meyer, C. Limberg) Springer, Berlin, Heidelberg, **2006**. For selected examples of alkene functionalization: a) J. H. Delcamp, A. P. Brucks, M. C. White, *J. Am. Chem. Soc.* **2008**, *130*, 11270–11271. b) R. J. DeLuca, M. S. Sigman, *J. Am. Chem. Soc.* **2011**, *133*, 11454–11457. c) Z. Liu, H.-Q. Ni, T. Zeng, K. M. Engle, *J. Am. Chem. Soc.* **2018**, *140*, 3223–3227. d) X. Yang, X. Li, P. Chen, G. Liu, *J. Am. Chem. Soc.***2022**, *144*, 7972–7977.

[22] a) H. Grennberg, A. Gogoll, J. E. Bäckvall, *Organometallics* **1993**, *12*, 1790–1793. b) X. Chen, J.-J. Li, X.-S. Hao, C. E. Goodhue, J.-Q. Yu, *J. Am. Chem. Soc.* **2006**, *128*, 78–79. c) K. L. Hull, M. S. Sanford, *J. Am. Chem. Soc.* **2009**, *131*, 9651–9653. d) C. A. Salazar, K. N. Flesch, B. E. Haines, P. S. Zhou, D. G. Musaev, S. S. Stahl, *Science* **2020**, *370*, 1454–1460. e) D. L. Bruns, D. G. Musaev, S. S. Stahl, *J. Am. Chem. Soc.* **2020**, *142*, 19678–19688.

[23] V. T. Tran, Z.-Q. Li, O. Apolinar, J. Derosa, S. R. Wisniewski, M. V. Joannou, M. D. Eastgate, K. M. Engle, *Angew. Chem. Int. Ed.* **2020**, *59*, 7409–7413. b) V. T. Tran, N. Kim, C. Z. Rubel, X. Wu, T. Kang, T. C. Jankins, Z.-Q. Li, M. V. Joannou, S. Ayers, M. Gembicky, J. Bailey, E. J. Sturgell, B. B. Sanchez, J. S. Chen, S. Lin, M. D. Eastgate, S. R. Wisniewski, K. M. Engle, *Angew. Chem. Int. Ed.* **2023**, *62*, e202211794. c) W.-J. He, W.-Z. Qin, S. Yang, S. Ma, N. Kim, J. E. Schultz, M. D. Palkowitz, C. He, A. Ma, M. A. Schmidt, M. Gembicky, S. R. Wisniewski, K. M. Engle, *ChemRxiv* **2024**. DOI: 10.26434/chemrxiv-2024-sj081.

[24] a) Y. Jang, V. N. G. Lindsay, *Org. Lett.* **2020**, *22*, 8872–8876. b) S. W. Reilly, Y. Lam, S. Ren, N. A. Strotman, *J. Am. Chem. Soc.* **2021**, *143*, 4817–4823. c) I. Y. Cho, W. G. Kim, J. H. Jeon, J. W. Lee, J. K. Seo, J. Seo, S. Y. Hong, *J. Org. Chem.* **2021**, *86*, 9328–9343. d) Y. Li, Q. Shao, H. He, C. Zhu, X.-S. Xue, J. Xie, *Nat. Commun.* **2022**, *13*, 10. e) S. Roediger, S. U. Leutenegger, B. Morandi, *Chem. Sci.* **2022**, *13*, 7914–7919. f) T. You, J. Li, *Org. Lett.* **2022**, *24*, 6642–6646. g) N. M. Orchanian, S. Guizzo, M. L. Steigerwald, C. Nuckolls, L. Venkataraman, *Chem. Commun.* **2022**, *58*, 12556–12559. h) S.-C. Tao, F.-C. Meng, T. Wang, Y.-L. Zheng, *Chem. Sci.* **2023**, *14*, 2040–2045.

[25] S. H. Cho, K. R. Wirtz, L. S. Liebeskind, *Organometallics* **2002**, *9*, 3067–3072. b) K. Chakarawet, T. D. Harris, J. R. Long, *Chem. Sci.* **2020**, *11*, 8196–8203.

[26] M. T. Huynh, C. W. Anson, A. C. Cavell, S. S. Stahl, S. Hammes-Schiffer, *J. Am. Chem. Soc.* **2016**, *138*, 15903–15910. b) T. Diao, Q. Lin, G. Dawson, *Synlett* **2021**, *32*, 1606–1620.

[27] S. Z. Tasker, T. F. Jamison, *J. Am. Chem. Soc.* **2015**, *137*, 9531–9534. b) A. de Aguirre, I. Funes-Ardoiz, F. Maseras, *Angew. Chem. Int. Ed.* **2019**, *58*, 3898–3902.

[28] A. M. Allgeier, C. A. Mirkin, *Angew. Chem. Int. Ed.* **1998**, *37*, 894–908. b) O. R. Luca, R. H. Crabtree, *Chem. Soc. Rev.***2013**, *42*, 1440–1459. c) V. Lyaskovskyy, B. de Bruin, *ACS Catal.* **2012**, *2*, 270–279.

[29] Y. Hwang, S. R. Wisniewski, K. M. Engle, *J. Am. Chem. Soc.* **2023**, *145*, 25293–25303.

[30] C. Z. Rubel, W.-J. He, S. R. Wisniewski, K. M. Engle, *Acc. Chem. Res.* **2024**, *57*, 312–326.

[31] R. Jain, K. Kabir, J. B. Gilroy, K. A. Mitchell, K. C. Wong, R. G. Hicks, *Nature* **2007**, *445*, 291–294.

[32] Deposition numbers 2304663 for Ni(dppe)(η^6-DQ) and 2304664 Ni(dppe)(η^2-DQ) contain the supplementary crystallographic data for this paper. These data are provided free of charge by the joint Cambridge Crystallographic Data Centre and Fachinformationszentrum Karlsruhe Access Structures service.

[33] J. M. Blacquiere, *ACS Catal.* **2021**, *11*, 5416–5437. b) A. F. Orsino, M.-E. Moret, *Organometallics* **2020**, *39*, 1998–2010. c) H. Shao, S. Chakrabarty, X. Qi, J. M. Takacs, P. Liu, *J. Am. Chem. Soc.* **2021**, *143*, 4801–4808. d) P. Font, H. Valdés, G. Guisado-Barrios, X. Ribas, *Chem. Sci.* **2022**, *13*, 9351–9360. e) P.-F. Wang, J. Yu, K.-X. Guo, S.-P. Jiang,

J.-J. Chen, Q.-S. Gu, J.-R. Liu, X. Hong, Z.-L. Li, X.-Y. Liu, *J. Am. Chem. Soc.* **2022**, *144*, 6442–6452.

[34] Conformational search was performed using CREST and GFN2-xTB. All low-energy conformers were then fully optimized by DFT at the (U)ωB97X-D/6-311+G(d,p)–SDD(Ni)/SMD(THF)//(U)B3LYP-D3(BJ)/6-31G(d)–SDD(Ni) level of theory. See SI for computational details.

[35] A. J. Foster, F. Weinhold, *J. Am. Chem. Soc.* **1980**, *102*, 7211–7218. b) J. Carpenter, F. Weinhold, *J. Mol. Struct. Theochem.* **1988**, *169*, 41–62.

[36] K. Chakarawet, T. D. Harris, J. R. Long, *Chem. Sci.* **2020**, *11*, 8196–8203.

[37] L. Tendera, T. Schaub, M. J. Krahfuss, M. W. Kuntze-Fechner, U. Radius, *Eur. J. Inorg. Chem.* **2020**, *33*, 3194–3207.

Entry for the Table of Contents

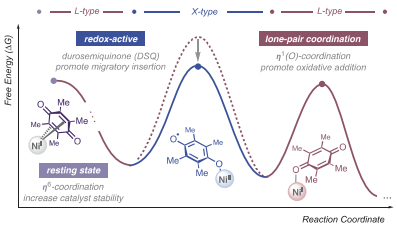

The redox-active quinone ligand enables seamless oxidation state manipulation between Ni(I) and Ni(II) intermediates, which facilitates the migratory insertion step. Meanwhile, the L-type lone-pair coordination promotes oxidative addition at a relatively more electron-rich Ni(I) center. These mechanistic discoveries enable the installation of alkylsulfenyl (–SAlkyl) groups in a series of 1,2-carbosulfenylation reactions of unactivated alkenes.

Twitter/X: @EngleLab @pengliu_group